A COMPARISON OF EIGENVALUE FOLLOWING ALGORITHMS APPLIED TO STRUCTURES WITH SYMMETRIC COMPLEX-VALUED STIFFNESS MATRICES

Miller, U.; Bograd, S.; Schmidt, A.; Gaul, L.
Institute of Applied and Experimental Mechanics, University of Stuttgart
Pfaffenwaldring 9, 70550 Stuttgart, Germany
miller@iam.uni-stuttgart.de

SUMMARY: A vibration analysis of a structure with joints is performed. The simulation is conducted with FE software capable of performing a numeric modal analysis with hysteretic damping ansatz. The joints are modeled with thin layer elements, representing dissipation and stiffness of the joints. The matrices describing the system consist of the mass, as well as real and complex-valued stiffness matrices. If the eigenvalues of this system are found in one step, due to the mode crossing occurring for the closely spaced modes, it is difficult and time consuming to assign modal damping factors to the corresponding undamped eigenvalues. In order to avoid this problem, the eigenvalue following method is used. The outcome of the solution is the graphical presentation of continuous eigenvalue paths, showing the change in the eigenvalues from the undamped to the fully damped case. For every undamped eigenvalue exists its equivalent eigenfrequency and damping factor that can be used for further numerical analysis.

In scope of this article a comparison of a Predictor-Corrector and Rayleigh-Quotient Iteration eigenvalue following algorithms, targeting specifically the type of matrices resulting from the weakly damped hysteretic formulation, is performed. The goal is to find a compromise between the accuracy and the processing speed, as well as to find the maximum reasonable size of a problem for a Matlab based solution.

KEYWORDS: Hysteretic Damping, Complex Eigenvalues, Path Following, Complex Stiffness Matrix

1 INTRODUCTION

Viscous damping is usually used for modeling of dissipation in Finite Element vibration analysis, because there exists a relatively simple mathematical model in time and frequency domain, which is well studied and is available in most FE codes. However, viscous damping is proportional to the velocity, so it increases with growing frequency, which is not a common behavior for most structures. Structures made out of metals containing joints have nearly frequency independent damping in most applications.

Another method to model vibration dissipation in structures is with hysteretic damping which is completely frequency independent. A constant damping factor (loss factor) is taken for the modeling of the dissipation in materials, and joints are modeled with thin layer elements representing equivalent dissipation and stiffness of the joints [8]. This method shows a better correlation with real life structures, however it can be used only in frequency domain, since in time domain it leads to non-causal material behavior [4, 11]. Since it is often needed to perform simulations in time domain, for example for transient analysis, the modal damping factors are calculated in frequency domain for each mode and then are used with the undamped eigenfrequencies and modes for further simulations. So it is necessary to have a table with undamped eigenfrequencies and corresponding modal damping factors. The problem, discussed in this article, occurs for structures with closely spaced modes, where it is possible that due to the different modal damping factors the undamped eigenfrequencies do not correspond to the damped eigenfrequencies — mode order changes, making a direct damping assignment difficult. Finding appropriate damping values for the eigenfrequencies can be done by visual comparison of the damped and undamped modes, but for complicated structures with many modes this method is quite tedious and time consuming. An alternative is to use the eigenpath following method to find the damping in the system. The results of the eigenpath calculation can be represented by a table or graphically by plotting real and imaginary

components of the complex eigenvalues versus the homotopy number, which is a number between zero and one, corresponding to the undamped and to the fully damped system respectively.

There exist numerous methods for pathfollowing algorithms. Two of them – Predictor-Corrector Method (PC) and Rayleigh Quotient Iteration (RQI) are tested in scope of this article [1]. The algorithms are implemented in Matlab and the system matrices as well as the undamped eigenvalues and eigenvectors are exported from MSC.Nastran. The goal is to see which method performs faster and gives better accuracy. Factors affecting both of these comparison parameters are also discussed. Since the calculations are performed in Matlab, which has a limit on the size of the matrices used, the maximum matrix size is also investigated.

2 Modelling of material and joint damping

It has been shown by experimental investigations that joint damping is nearly frequency independent [5, 6, 7]. Similar results have been shown for material damping in metals, where the main cause of dissipation is inner friction in the material [12, 18, 20]. So for FE modeling the principle of constant hysteresis will be used. Such model makes sense only in frequency domain, while in time domain it leads to non-causal material behavior [4, 11]. Some investigations to this model have been made already and show a good correlation with experimentally determined joint parameters [10, 13, 14].

During the calculation of the vibrational characteristics of the structure with the FEM the following equation of motion for an undamped system is used

$$\boldsymbol{M}\,\ddot{\boldsymbol{u}} + \boldsymbol{K}\,\boldsymbol{u} = \boldsymbol{0}\,, \tag{1}$$

where $\boldsymbol{M}$ and $\boldsymbol{K}$ are symmetric real-valued $n \times n$ mass and stiffness matrices, and $\boldsymbol{u}$ is the displacement vector. An exponential ansatz $\boldsymbol{u}_i = \boldsymbol{\phi}_i e^{\lambda_i t}$ leads to an eigenvalue problem

$$(\boldsymbol{M}\,\lambda_i^2 + \boldsymbol{K})\boldsymbol{\phi}_i = \boldsymbol{0}\,. \tag{2}$$

Eigenvalues and eigenmodes can be determined by performing a numerical modal analysis with a standard FE software. Using the principle of constant hysteresis, the damping will be incorporated into the stiffness matrix by augmenting it with the complex-valued product of experimentally determined dissipation multipliers α_i and β_i for the material and the joint damping, respectively, and the associated elements stiffness matrices

$$\boldsymbol{K}^* = \boldsymbol{K} + \mathrm{j}\,\boldsymbol{D} = \boldsymbol{K} + \mathrm{j}\sum \alpha_i \boldsymbol{K}_i^{(\mathrm{Material})} + \mathrm{j}\sum \beta_i \boldsymbol{K}_i^{(\mathrm{Joint})}\,. \tag{3}$$

For the considered systems, damping is low and $\alpha_i\,, \beta_i \ll 1$ holds. The solution of the complex-valued system

$$(\boldsymbol{M}\,\lambda_i^2 + \mathrm{j}\boldsymbol{D} + \boldsymbol{K})\boldsymbol{\phi}_i = (\boldsymbol{M}\,\lambda_i^2 + \boldsymbol{K}^*)\boldsymbol{\phi}_i = \boldsymbol{0} \tag{4}$$

leads to complex eigenvalues $\lambda_i = \delta_i + \mathrm{j}\omega_i$ and eigenvectors $\boldsymbol{\phi}_i = \boldsymbol{r}_i e^{\mathrm{j}\kappa_i}$. The solution vector represented by an exponential ansatz may be written as

$$\boldsymbol{u}_i = \boldsymbol{\phi}_i e^{\lambda_i t} = \boldsymbol{r}_i e^{\mathrm{j}\kappa_i} e^{\lambda_i t} = \boldsymbol{r}_i e^{\delta_i t + \mathrm{j}(\omega_i t + \kappa_i)}\,, \tag{5}$$

where $\boldsymbol{r}_i$ is the amplitude of vibration, δ_i is the modal damping, ω_i and κ_i are the frequency and phase shift, respectively.

This modified equation of motion can be solved for complex eigenvalues and eigenmodes with some commercial FE packages, and in this case was performed with Nastran. The modal damping factors of the structure are read out from the solution.

3 Path Following

A transient or an operational vibration analysis of mechanical systems often requires a correspondence between the damped and the undamped eigenvalues to assign modal damping to the undamped eigenmodes. For systems with high mode density, it is difficult to find this correspondence if the damped system is solved in one step without any relation to the undamped one.

To find this mapping between the eigenvalues, a so called homotopy parameter μ is introduced so that the solution can follow the eigenvalues from the undamped system at $\mu = 0$ to the damped system at $\mu = 1$ [1]. Then the calculated paths can be constructed, showing clearly where the modes cross each other. In addition, the sensitivity of the calculated modal damping factors may be analyzed [19]. Alternatively, a text file with a table containing undamped eigenvalues and modal damping factors can be exported and read into the Nastran or other commercial FE solvers and used for further analysis.

The system equation of motion (4) with homotopy parameter μ has the following form

$$(\boldsymbol{M}\,\lambda_i^2 + \mu \mathrm{j}\boldsymbol{D} + \boldsymbol{K})\boldsymbol{\phi}_i = \boldsymbol{0}\ , \quad 0 \le \mu \le 1\ , \tag{6}$$

where λ_i und $\boldsymbol{\phi}_i$ are the complex eigenvalues and corresponding eigenvectors of the system which coincide with the eigenvalues and eigenvectors of the undamped system for $\mu = 0$ [2, 3]. Now the path following, also known as the numeric continuation method is implemented. Based on the undamped system at $\mu = 0$, the homotopy parameter is increased step by step and the eigenvalue problem (6) is solved.

There are two different methods described in this article. First method shown – the Predictor-Corrector Method – is based on the initial prediction of the desired solution of the eigenvalue problem and then it uses Newton's method to correct it to achieve appropriate accuracy. Afterward, the Rayleigh Quotient Iteration is presented which is a widely used iterative method to compute eigenvalues and eigenvectors of symmetric systems.

3.1 Predictor-Corrector Method

Because the eigenvectors can be scaled arbitrarily, the eigenvalue problem (6) is expanded by a suitable scaling equation

$$\begin{bmatrix} (\boldsymbol{M}\lambda_i^2 + \mathrm{j}\,\mu\boldsymbol{D} + \boldsymbol{K})\boldsymbol{\phi}_i \\ \boldsymbol{\phi}_{i\,0}^H\,\boldsymbol{\phi}_i \end{bmatrix} = \begin{bmatrix} \boldsymbol{0} \\ 1 \end{bmatrix}\ , \tag{7}$$

with the starting eigenvalue $\boldsymbol{\phi}_{i\,0}$ (for $\mu = 0$). If the eigenpair $(\boldsymbol{\phi}_i, \lambda_i)$ is denoted by a vector

$$\boldsymbol{z}_i = \begin{bmatrix} \boldsymbol{\phi}_i \\ \lambda_i \end{bmatrix}\ , \tag{8}$$

then Equation (7) can be written as

$$\boldsymbol{g}(\boldsymbol{z}_i(\mu), \mu) = \begin{bmatrix} \boldsymbol{g}_1 \\ g_2 \end{bmatrix} = \begin{bmatrix} (\boldsymbol{M}\lambda_i^2 + \mathrm{j}\,\mu\boldsymbol{D} + \boldsymbol{K})\boldsymbol{\phi}_i \\ \boldsymbol{\phi}_{i\,0}^H\boldsymbol{\phi}_i - 1 \end{bmatrix} = \boldsymbol{0}\,. \tag{9}$$

This equation depends nonlinearly on λ_i, and is solved with the help of the Predictor-Corrector Formulation (PC) with the ansatz

$$\boldsymbol{g}(\boldsymbol{z}_i(\mu), \mu) = \boldsymbol{g}(\bar{\boldsymbol{z}}_i(\mu), \bar{\mu}) + \boldsymbol{g}_{,\boldsymbol{z}}\big|_{\bar{\boldsymbol{z}}_i, \bar{\mu}}\,\Delta\boldsymbol{z} = \boldsymbol{0}\,, \tag{10}$$

where $\bar{\boldsymbol{z}}_i, \bar{\mu}$ are known values and $\circ_{,x}$ are derivatives with respect to different values of x [19]. The required derivatives are

$$\boldsymbol{g}_{1,\boldsymbol{\phi}_i} = \lambda_i^2\boldsymbol{M} + \mathrm{j}\,\mu\boldsymbol{D} + \boldsymbol{K} \tag{11}$$

$$\boldsymbol{g}_{1,\lambda_i} = 2\lambda_i\boldsymbol{M}\boldsymbol{\phi}_i \tag{12}$$

$$g_{2,\boldsymbol{\phi}_i} = \boldsymbol{\phi}_i^{\mathrm{H}} \tag{13}$$

$$g_{2,\lambda_i} = 0\,. \tag{14}$$

Differentiating Equation (9) with respect to μ leads to

$$\boldsymbol{g}_{,\mu} = \boldsymbol{g}_{,\boldsymbol{z}}\boldsymbol{z}_{,\mu} = \begin{bmatrix} \boldsymbol{g}_{1,\boldsymbol{\phi}_i} & \boldsymbol{g}_{1,\lambda_i} \\ \boldsymbol{g}_{2,\boldsymbol{\phi}_i} & g_{2,\lambda_i} \end{bmatrix} \begin{bmatrix} \boldsymbol{\phi}_{i,\mu} \\ \lambda_{i,\mu} \end{bmatrix}, \tag{15}$$

and Equation (10) reformulated yields

$$\boldsymbol{g}_{,\boldsymbol{z}}\big|_{\bar{\boldsymbol{z}}_i, \bar{\mu}}\,\Delta\boldsymbol{z} = \begin{bmatrix} \boldsymbol{g}_{1,\boldsymbol{\phi}_i} & \boldsymbol{g}_{1,\lambda_i} \\ \boldsymbol{g}_{2,\boldsymbol{\phi}_i} & g_{2,\lambda_i} \end{bmatrix} \Delta\boldsymbol{z} = -\begin{bmatrix} \boldsymbol{g}_1 \\ g_2 \end{bmatrix}\ . \tag{16}$$

For the predictor step, the derivation

$$\boldsymbol{g}_{,\mu} = \begin{bmatrix} (2\lambda_i\lambda_{i,\mu}\boldsymbol{M} + \mathrm{j}\boldsymbol{D})\boldsymbol{\phi}_i + (\lambda_i^2\boldsymbol{M} + \mathrm{j}\mu\boldsymbol{D} + \boldsymbol{K})\boldsymbol{\phi}_{i,\mu} \\ \boldsymbol{\phi}_{i\,0}^{\mathrm{H}}\boldsymbol{\phi}_{i,\mu} \end{bmatrix} = \boldsymbol{0} \tag{17}$$

is used, which leads to

$$\begin{bmatrix} \boldsymbol{g}_{1,\boldsymbol{\phi}_i} & \boldsymbol{g}_{1,\lambda_i} \\ \boldsymbol{g}_{2,\boldsymbol{\phi}_i} & 0 \end{bmatrix} \boldsymbol{z}_{,\mu} = \begin{bmatrix} -(\boldsymbol{K} + \mathrm{j}\boldsymbol{D})\boldsymbol{\phi}_i \\ 0 \end{bmatrix}. \tag{18}$$

Equation (7) can be solved iteratively for the actual homotopy parameter

$$\mu_{n+1} = \mu_n + h \tag{19}$$

with predictor

$${}^{n+1}\boldsymbol{z}_i = {}^{n}\boldsymbol{z}_i + h \cdot {}^{n}\boldsymbol{z}_{\,i,\mu} \tag{20}$$

calculated from equation (18). Then the result is corrected with Newton's Method from Equation(16)

$${}^{n+1}\boldsymbol{z}_i^{(t+1)} = {}^{n+1}\boldsymbol{z}_i^{(t)} + \Delta\boldsymbol{z}\,, \qquad t = 1, 2\,, \ldots \tag{21}$$

until the residual reaches a set convergence parameter.

3.2 Rayleigh-Quotient Iteration

If $\boldsymbol{K}$ and $\boldsymbol{M}$ are real symmetric $n \times n$ matrices and $\boldsymbol{\phi}$ is a given vector of dimension n, then the Rayleigh-Quotient of $\boldsymbol{\phi}$ is defined as [9, 15, 17]

$$r(\boldsymbol{\phi}) \equiv \frac{\boldsymbol{\phi}^T\boldsymbol{K}\boldsymbol{\phi}}{\boldsymbol{\phi}^T\boldsymbol{M}\boldsymbol{\phi}}\,. \tag{22}$$

If $\boldsymbol{\phi}_0$ is an approximation to an eigenvector of the generalized eigenvalue problem $\boldsymbol{K}\boldsymbol{\phi} = \lambda\boldsymbol{M}\boldsymbol{\phi}$, then $r(\boldsymbol{\phi}_0)$ can be used to find an approximation to the corresponding eigenvalue λ_0. Alternatively, the problem can be solved for the eigenvector, if there exists an approximate value λ_0, then the solution of

$$(\boldsymbol{K} - \lambda_0\boldsymbol{M})\boldsymbol{\phi}_0 = \boldsymbol{b} \tag{23}$$

is almost always a good choice for the eigenvector of the generalized eigenvalue problem [9]. Also, Equation (23) can be solved with a suitable assigned approximation to the eigenvector for the right hand side $\boldsymbol{b}$ (e.g.: undamped eigenvector for the damped problem). In case there is no approximate eigenvector available, one can choose a random vector, but it can lead to divergence and long solution times.

These two ideas are combined and adjusted to fit the available problem with symmetric real matrix $\boldsymbol{M}$ and complex matrix $\boldsymbol{K}$ to the Rayleigh-Quotient Iteration algorithm (RQI). The starting vector $\boldsymbol{\phi}_0$ from the undamped eigenvalue solution with $\|\boldsymbol{\phi}_0\| = 1$ is taken. Now iterating for $k = 0, 1, \ldots$ using Equation (22) the eigenvalue

$$\lambda_k = r(\boldsymbol{\phi}_k) \tag{24}$$

is found. In the next step equation

$$(\boldsymbol{K} - \lambda_k\boldsymbol{M})\boldsymbol{z}_{k+1} = \boldsymbol{\phi}_k \tag{25}$$

is solved for $\boldsymbol{z}_{k+1}$. The approximation of the eigenvector from the previous iteration, starting with $\boldsymbol{\phi}_0$, is taken for the right hand side of the Equation (25). Then the solution is normalized

$$\boldsymbol{\phi}_{k+1} = \boldsymbol{z}_{k+1}/\|\boldsymbol{z}_{k+1}\|\,. \tag{26}$$

The norm of the computed vector $\|\boldsymbol{z}_{k+1}\|$ increases while iterating and serves as a convergence criterion.

Unfortunately, the algorithm sometimes has problems to converge to the eigenvalue next to the start value λ_0 [16]. In order to avoid this problem for the path following algorithm the number of the homotopy steps can be increased and the eigenvector from the last homotopy step is taken as a starting vector.

4 Application and Results

4.1 Test Structures

The initial idea was to test both algorithms on a structure shown in Figure 1. The structure is made out of two 3 mm thick steel plates joined by bolts. In this case the joints are modeled with thin layer elements with constant damping. Since steel has very low damping and no macro-slip occurs in the joints, damping of the assembly for the first ten modes is lower than 0.2 %. The structure is modeled with brick elements and has 76 800 degrees of freedom. The undamped eigenvalues and eigenmodes are found with Nastran and exported into ASCII files together with mass, stiffness, and damping matrices. The exported matrices are imported into Matlab in sparse format, but due to the large number of elements the software shows an "out of memory" error. No further data manipulation, like using binary format or exporting sparse matrices direct out of Nastran, was performed in time for this paper. With the current process chain, data input algorithms are the limiting factor for the size of matrices. Up to circa 50 000 DOFs the matrices could be read into Matlab.

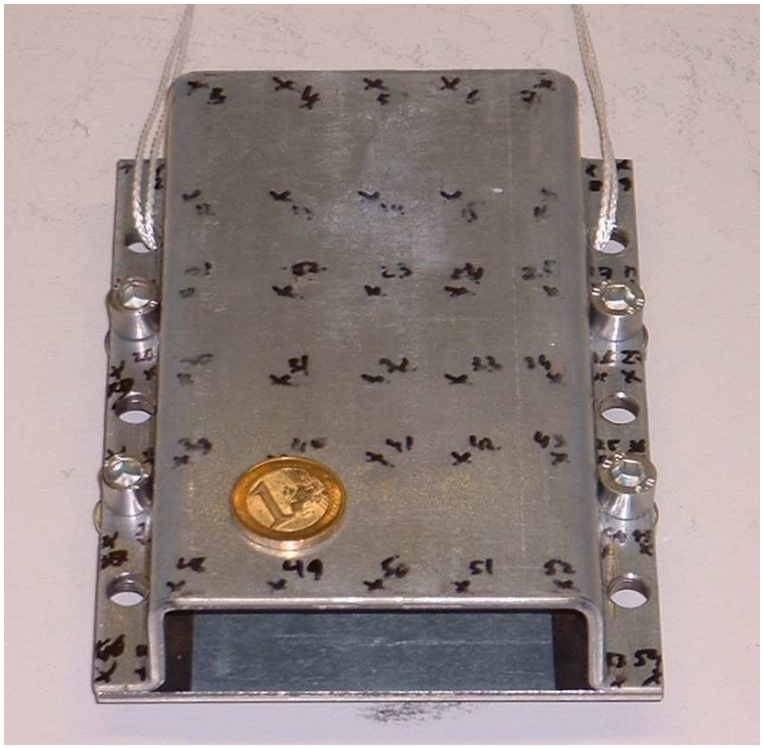

Figure 1: Test structure

Two smaller models shown in Figure 2 were created for purposes of analyzing computing speed and accuracy of the algorithms. Model 1, shown on the left, has 13872 DOFs, half of which are rotational and are equal to zero. After all zero DOFs are removed the problem has 6936 DOFs. Model 2, shown on the right, is exactly 2 times smaller – it has 3468 DOFs. Also, a small model with 164 DOFs and many closely spaced modes used to check the reliability of the algorithms was generated. Figure 3 shows an example of an eigenpath following for this small model. The paths of modes 3 and 4 cross each other because of the significantly different damping values, as it can be seen on the right side of the figure.

4.2 Computational Time and Accuracy

Calculations were performed on a 3.0 GHz dual core processor with 16 GB RAM. Only one processor core was used for each Matlab calculation. 20 modes were found for each model and average time in seconds per one mode are shown in Table 1. As expected RQI method is much faster, since it uses only matrix-vector operations. PC on the other hand uses matrix inversion, making the calculation times significantly

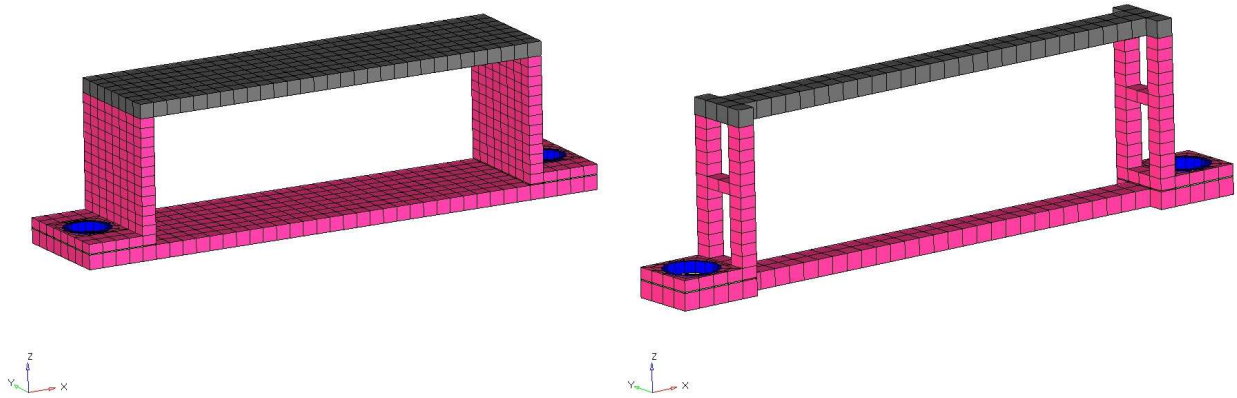

Figure 2: FE models with 6936 and 3468 DOFs used for algorithms testing

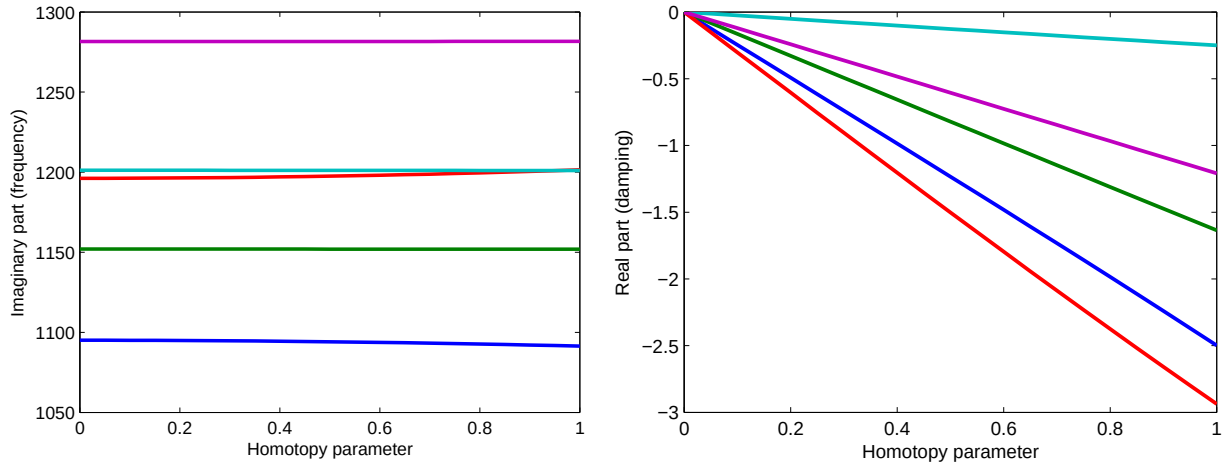

Figure 3: Imaginary and real part of five eigenvalues of the 164 DOF model

longer. Also, the solution time for the RQI algorithm increases quadratically with increase of DOFs and cubically for the PC method. No difference in time is noticed for the calculation of the eigenvalues for closely spaced modes and for those located far apart from each other.

Algorithm	Model 1 (Seconds)	Model 2 (Seconds)
Predictor-Corrector	93860	14480
Rayleigh Quotient	6	2.1

Table 1: Computional times for *one* mode for both models and algorithms

Apart from the differences resulting from non-identical matrix operations, an important role in computational time plays the accuracy of the results, which in turn is dependent on the convergence criterion – residual error and number of homotopy steps needed for the problem to converge and to give appropriate accuracy.

The benchmark solution is performed with complex eigenvalue solver in Nastran. Both algorithms showed nearly identical results with less than 0.5 % difference between the Nastran and Matlab values.

5 Conclusions

This article gives a short overview and comparison of two eigenvalue following algorithms: Predictor-Corrector (PC) and Rayleigh-Quotient Iteration (RQI). Both algorithms are applied to a weakly damped FE model with hysteretic damping. The PC method employs matrix inversion operations in order to find the solution, whereas RQI uses only matrix-vector operations, making the computational speed proportional to n^3 for the PC method and n^2 for the RQI method. This makes RQI method significantly faster than PC, especially for large problems, where the later one is prohibitively time consuming.

The accuracy of both methods depends on the convergence criterion, with higher accuracy usually resulting in higher computational times. Generally, both methods show good results within 0.5 % from the Nastran solution values.

The biggest limitation though, is the data transfer between the FE software and Matlab, with later one having difficulties processing matrices with more then $50\,000 \times 50\,000$ elements. Some of the possible solutions are writing the matrices out of the FE in sparse format and preferably in binary and not ASCII files. However, most likely if the systems with over 1 000 000 DOFs will be used, the algorithms should be implemented in C or Fortran programming languages, and Matlab can be used for a quick algorithm testing and modification.

6 Acknowledgment

The support of the project "Experimentelle Ermittlung von Kennwerten zur Werkstoff- und Fügestellendämpfung sowie deren Berücksichtigung in Finite-Elemente-Berechnungen" by the Forschungsvereinigung für Verbrennungskraftmaschinen (FVV) and Deutsche Forschungsgemeinschaft (DFG) which enabled us to perform these investigations is gratefully acknowledged.

References

[1] E. L. Allgower and K. Georg. *Introduction to Numerical Continuation Methods.* SIAM, 2003.

[2] I. Bar-on and M Paprzycki. High performance solution of the complex symmetric eigenproblem. *Numerical Algorithms*, 18:195–208, 1998.

[3] F. Cortes and M. J Elejabarrieta. An approximate numerical method for the complex eigenproblem in systems characterised by a structural damping matrix. *Journal of Sound and Vibration*, 296:166–182, 2006.

[4] S. Crandall. The role of damping in vibration theory. *Journal of Sound and Vibration*, 11:3–18, 1970.

[5] D Ewins. *Modal Testing: theory, practice and application.* Research Studies Press, 2nd edition, 2000.

[6] L. Garibaldi and H. N Onah. *Viscoelastic Material Damping Technology.* Beccis Osiride, 1996.

[7] L. Gaul and R. Nitsche. The role of friction in mechanical joints. *Applied Mechanics Reviews*, 54:93–106, 2001.

[8] L. Gaul, A. Schmidt, and S. Bograd. Experimentelle ermittlung von kennwerten zur werkstoff- und fügestellendämpfung sowie deren berücksichtigung in finite-elemente-berechnungen. Forschungsvereinigung Verbrennungskraftmaschinen Heft (FVV) 859, Frankfurt, 2008.

[9] Gene H. Golub and Charles F. Van Loan. *Matrix Computations.* Johns Hopkins University Press, 1986.

[10] D. J Henwood. Approximating the hysteretic damping matrix by a viscous matrix for modeling in the time domain. *Journal of Sound and Vibration*, 254:575–593, 2002.

[11] J. A. Inaudi and N. Makris. Time-domain analysis of linear hysteretic damping. *Earthquake Engineering and Structural Dynamics*, 25:529–545, 1996.

[12] R. S Lakes. *Viscoelastic Solids*. CRC Press, 1999.

[13] Ahid D. Nashif, David I.G. Jones, and John P Henderson. *Vibration Damping*. John Wiley and Sons, 1985.

[14] D. Ottl. Schwingungen mechanischer systeme mit strukturdämpfung. VDI- Forschungsheft 603, 1981.

[15] Beresford N. Parlett. The rayleigh quotient iteration and some generalizations for nonnormal matrices. *Mathematics of Computation*, 28(127):679–693, 1974.

[16] Beresford N. Parlett. *The Symmetric Eigenvalue Problem*, volume 20 of *Classics In Applied Mathematics*. SIAM, 1998.

[17] Axel Ruhe. Computation of eigenvalues and eigenvectors. In Vincent Allan Barker, editor, *Sparse Matrix Techniques*, pages 130–184. Springer-Verlag, 1977.

[18] A. Schmidt and L. Gaul. On the numerical evaluation of fractional derivatives in multi-degree-of-freedom systems. *Signal Processing*, 86:2592–2601, 2006.

[19] N. Wagner and L. Gaul. Eigenpath analyses of friction induced vibrations depending on the friction coefficient. *PAMM*, 3:130–131, 2003.

[20] A. Wineman and K. R. Rajagopal. *Mechanical Response of Polymers*. University Press, 2000.